Differently anchored influenza hemagglutinin mutants display distinct interaction dynamics with mutual rafts

Dmitry E. Shvartsman,[1] Mariana Kotler,[1] Renee D. Tall,[2] Michael G. Roth,[2] and Yoav I. Henis[1]

[1]Department of Neurobiochemistry, George S. Wise Faculty of Life Sciences, Tel Aviv University, Tel Aviv 69978, Israel
[2]Department of Biochemistry, University of Texas Southwestern Medical Center, Dallas, TX 75235

L ipid rafts play important roles in cellular functions through concentrating or sequestering membrane proteins. This requires proteins to differ in the stability of their interactions with lipid rafts. However, knowledge of the dynamics of membrane protein–raft interactions is lacking. We employed FRAP to measure in live cells the lateral diffusion of influenza hemagglutinin (HA) proteins that differ in raft association. This approach can detect weak interactions with rafts not detectable by biochemical methods. Wild-type (wt) HA and glycosylphosphatidyl-inositol (GPI)-anchored HA (BHA-PI) diffused slower than a nonraft HA mutant, but became equal to the latter after cholesterol depletion. When antigenically distinct BHA-PI and wt HA were coexpressed, aggregation of BHA-PI into immobile patches reduced wt HA diffusion rate, suggesting transient interactions with BHA-PI raft patches. Conversely, patching wt HA reduced the mobile fraction of BHA-PI, indicating stable interactions with wt HA patches. Thus, the anchoring mode determines protein–raft interaction dynamics. GPI-anchored and transmembrane proteins can share the same rafts, and different proteins can interact stably or transiently with the same raft domains.

Introduction

Lipid rafts, membrane microdomains enriched in cholesterol and glycosphingolipids, are involved in diverse cellular functions such as transmembrane (TM) signaling and apical sorting in polarized epithelial cells (Simons and Ikonen, 1997; Kurzchalia and Parton, 1999; Smart et al., 1999; Brown and London, 2000; Simons and Toomre, 2000; Anderson and Jacobson, 2002). They also play important roles in pathophysiological processes such as formation of infectious scrapie or generation of β-amyloid in Alzheimer's disease (Prusiner, 1998; Kurzchalia and Parton, 1999; Smart et al., 1999; Ehehalt et al., 2003). Lipid rafts are thought to function as scaffolds that either concentrate or segregate interacting proteins. However, their composition, size, and the extent to which proteins stably interact with them in biological membranes are poorly understood.

Proteins that interact with lipid rafts are often identified by their ability to be floated in vitro on gradients with detergent-resistant membranes (DRMs) from cells lysed in nonionic detergents (typically Triton X-100) at 4°C (Simons and Ikonen, 1997; Brown and London, 2000). Although this

method identifies proteins capable of a fairly stable interaction with lipid rafts, it is unclear how strong these interactions must be to allow isolation in DRMs. In addition, there is evidence for the existence of more than one type of lipid raft. Caveolae, morphologically distinct membrane invaginations containing caveolin/VIP21 (Kurzchalia et al., 1992; Rothberg et al., 1992), are a specialized form of raft, but rafts exist also in cells lacking caveolae (Kurzchalia and Parton, 1999; Smart et al., 1999; Brown and London, 2000; Simons and Toomre, 2000; Anderson and Jacobson, 2002). The immunological synapse in T cells may also be considered a specific type of lipid raft that binds to the actin cytoskeleton (Grakoui et al., 1999; Janes et al., 1999; Zhang and Samelson, 2000). The sensitivity of proteins in different types of rafts to detergent extraction has not been systematically compared. Adding complexity to this situation, membrane fractions soluble in Triton X-100, but not in another nonionic detergent, have been reported and equated with a subpopulation of lipid rafts of distinct composition existing in biological membranes (Roper et al., 2000). In intact cells, FRET studies of acylated GFP derivatives in the cytoplasmic leaflet of the plasma membrane suggest that they cluster in more than one lipid microdomain type (Zacharias et al., 2002). Determining the relationships between the isolation

of specific proteins with DRMs, their affinities to lipid rafts in intact cells and their biological activities, requires measurement of lipid raft association in living cells.

Several biophysical methods have been employed to measure raft association in cells and yielded variable results (Kurzchalia and Parton, 1999; Simons and Toomre, 2000; Anderson and Jacobson, 2002), probably due to the different parameters measured by each method. Thus, FRET studies yielded results either in favor (Varma and Mayor, 1998; Zacharias et al., 2002) or against (Kenworthy and Edidin, 1998; Kenworthy et al., 2000) the existence of rafts in live cells. Other methods (chemical cross-linking, single particle tracking, and laser trap) detected clustering of raft proteins in submicron domains, but yielded highly variable estimates of domain sizes (Friedrichson and Kurzchalia, 1998; Pralle et al., 2000; Anderson and Jacobson, 2002). These studies did not investigate the dynamics of protein–raft interactions (stable or transient association). This issue is important, as some hypotheses of the biological functions of lipid rafts implicitly require stable interaction of signaling molecules with rafts and others require the opposite. Recent studies on the dynamics of raft association have been limited to proteins in highly organized specialized raft structures, such as caveolin-1 in caveolae and LAT (linker for activation of T cells) in the T cell immunological synapse; these proteins were found to be laterally immobile in these structures (Thomsen et al., 2002, Tanimura et al., 2003).

Here we employed a combination of FRAP and immunofluorescence co-patching to investigate the raft association dynamics of influenza HA mutants bearing different (or no) raft-targeting signals. In epithelial cells, sorting of HA to the apical surface depends critically on its TM sequence, in correlation with its partitioning into Golgi-derived DRMs (Skibbens et al., 1989; Scheiffele et al., 1997; Lin et al., 1998). The availability of TM point mutants of HA that are excluded from DRMs (Scheiffele et al., 1997; Lin et al., 1998) makes the HA system ideal for studies on raft association, as it enables direct comparison between proteins that do or do not partition into rafts but are otherwise similar, excluding possible effects of other interactions. Moreover, comparison with a glycosylphosphatidylinositol (GPI)-anchored HA (BHA-PI; Kemble et al., 1994) allows us to measure differences between two mutants of the same protein that are targeted to rafts by different signals. Our studies demonstrate that the lateral diffusion rate of raft-associated HA proteins is retarded relative to a nonraft mutant in a cholesterol-dependent manner. Using a combination of
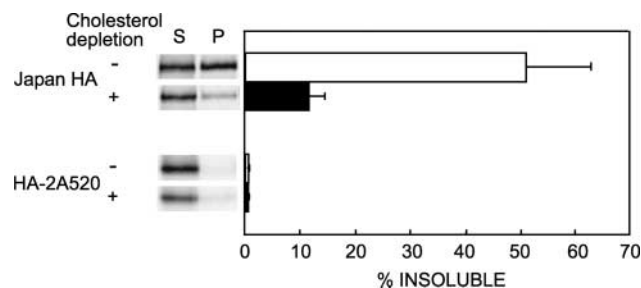
Figure 1. **Triton insolubility of HA mutants.** Experiments were conducted on Fugene 6–transfected COS-7 cells expressing Japan wt HA or Japan HA-2A520. Similar results (not depicted) were obtained on CV-1 cells infected with recombinant SV40 virus vectors. 24 h after transfection, the cells were subjected to cholesterol depletion as described under the Materials and methods. The cells were then labeled with [^{35}S]methionine and cysteine, chased 100 min in serum-free DME, and lysed 20 min on ice in 1 ml lysis buffer containing 1% Triton X-100. The lysates were separated into soluble and insoluble fractions by centrifugation, and these were immunoprecipitated with rabbit α-Japan HA antibody and analyzed by PAGE and phosphorimaging. Bars show the average ± SD of three to five replicates.

patching and FRAP studies, we show that a GPI-anchored HA and wild-type (wt) HA reside in mutual rafts, but differ in their mode of interaction with the raft domains (stable association for GPI-anchored proteins, and transient interactions for wt HA). The high sensitivity of this in vivo method allowed us to detect interactions with lipid rafts that are too weak for partitioning in DRMs in vitro but are sufficient to enable sorting to the apical surface.

Results

Cholesterol-sensitive retardation of the lateral diffusion of raft-associated HA proteins

The HA system is suitable for studies on the interactions of proteins with lipid rafts, due to the availability of mutants that differ in DRM partitioning and in their ability to undergo apical sorting in polarized cells, a process thought to require HA to enter lipid rafts (Scheiffele et al., 1997; Lin et al., 1998; Melkonian et al., 1999). Here we employed several such mutants derived from Japan HA (Table I) and compared their behavior at the surface of living cells (untreated or manipulated to reduce the cholesterol level). To demonstrate that the conditions employed to lower cholesterol affected (or not) the ability of the HA TM mutants expressed

Table I. **Japan HA mutants**

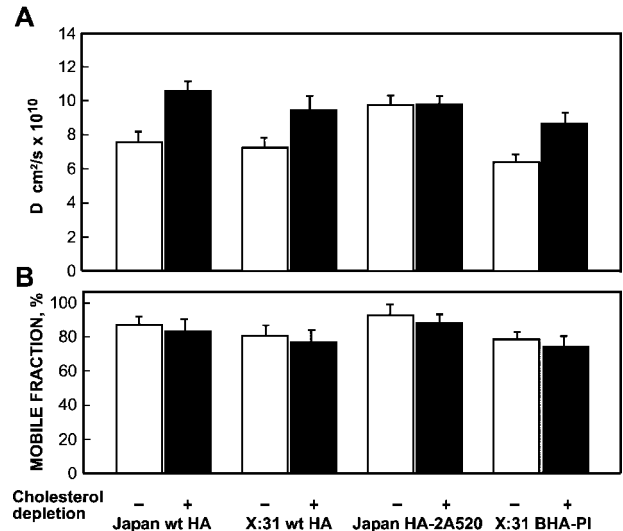| Japan HA mutant	Transmembrane sequence	Percent insoluble
wt HA	ILAIYATVAGSLSLAIMMAGISFWM	51 ± 12
HA-2A520	·········AA···············	0.6 ± 0.3
TM 11.0	··LL·········LLLLLLLLLLLLL	6 ± 4
TM 12.0	··LL·········LLLLLLLLLLLLL	36 ± 8

Mutations in the Japan HA TM domain. Amino acid sequences are depicted in single letter code beginning with the first residue of the TM domain (Ile511). Dots represent no change from the sequence of Japan wt HA. HA-2A520 was described earlier (Scheiffele et al., 1997; Lin et al., 1998). TM 11.0 and TM 12.0 are Japan HA mutants where stretches of the TM sequence were replaced with leucines (Alonso, M.A., personal communication; unpublished data). The percent insoluble column depicts the percentage of each protein that is insoluble in cold 1% Triton X-100 (averages ± SD of three experiments); values for wt HA and HA-2A520 are from Fig. 1.
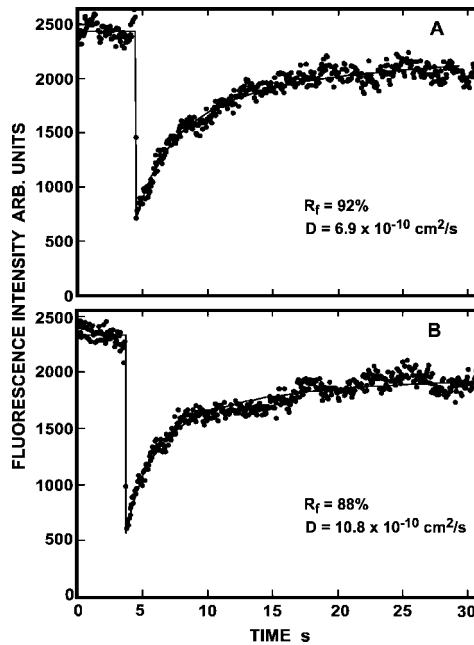
Figure 2. **Representative FRAP curves measuring the lateral diffusion of Japan wt HA.** CV-1 cells were infected with recombinant SV40 virions encoding Japan wt HA. After 16–18 h, the cells were either subjected to cholesterol depletion for 18–20 h, or left untreated for the same period. 36 h after infection, cell surface HAs were labeled with α-Japan TRITC-Fab' (100 μg/ml, 45 min, 4°C), and FRAP studies were conducted at 22°C. Solid lines are the best fit to the lateral diffusion equation using nonlinear regression (Fire et al., 1995). The lateral diffusion coefficients (D) and mobile fraction values (R_f) for each curve are shown. (A) Japan wt HA diffusion in an untreated cell. (B) Japan wt HA diffusion in a cholesterol-depleted cell.

Figure 3. **Cholesterol depletion elevates the lateral diffusion rates of DRM-associated HAs to the level of the nonraft HA-2A520.** The experiments were performed as in Fig. 2, on CV-1 cells infected with recombinant SV40 virions (36 h after infection) or transiently transfected with the relevant SV40 expression vectors encoding each HA mutant (48 h after transfection). Analogous experiments were conducted on COS-7 cells transiently transfected with the same vectors (24 h after transfection). In all cases, these incubation periods include 18–20-h cholesterol depletion treatment where applicable. Similar results were obtained on both cell types. Cell surface HAs were labeled with monovalent Fab' (100 μg/ml α-Japan TRITC-Fab' for Japan HAs, or 50 μg/ml α-X:31 rabbit Fab' followed by 50 μg/ml GαR TRITC-Fab' for X:31 HAs). Each bar is the mean ± SEM of 30–40 measurements. (A) D values. D of Japan HA-2A520 on untreated cells was significantly higher than D of wt HA (Japan or X:31) or of X:31 BHA-PI ($P < 0.001$). The effects of cholesterol depletion on the D values of the wt HAs ($P < 0.001$) and X:31 BHA-PI ($P < 0.01$) were significant; D of Japan HA-2A520 was not significantly affected by this treatment ($P > 0.25$). (B) Mobile fraction (R_f) values. There were no significant differences between the R_f values of Japan wt HA and Japan HA-2A520 ($P > 0.1$), or between X:31 wt HA and X:31 BHA-PI ($P > 0.25$). The R_f values were slightly reduced after cholesterol depletion, but this effect was not significant in all cases ($P > 0.05$) and was observed also for the Japan HA-2A520 mutant.

in our cells to associate with DRMs, we employed extraction with 1% Triton X-100 at 4°C (Lin et al., 1998; Melkonian et al., 1999; see Materials and methods). A portion of Japan wt HA, which is known to be raft resident, was insoluble in cold Triton X-100, whereas the nonraft mutant Japan HA-2A520 was nearly fully soluble (Fig. 1). Moreover, cholesterol depletion with compactin and mevalonate (Hua et al., 1996; Lin et al., 1998), which reduced the membrane cholesterol content by 30–35% (as determined by the F-CHOL kit; Boehringer), strongly reduced the Triton X-100–insoluble fraction of wt HA and had no effect on the mutant.

An important advantage of the HA system for biophysical studies on raft association is that HA lacks signals for internalization (Lazarovits and Roth, 1988) or for interaction with intracellular structures; its short cytoplasmic tail also reduces the potential for steric interactions with the fence-like membrane-associated cytoskeleton (Kusumi and Sako, 1996). These features minimize the possible masking of raft-related changes in HA mobility by other interactions. To determine the effect of partitioning into rafts on HA mobility, we employed FRAP to measure the lateral diffusion of wt HA or GPI-anchored BHA-PI (proteins demonstrated to associate with DRMs) relative to an HA mutant (HA-2A520) that is excluded from DRMs and is sorted preferentially to the basolateral surface in MDCK cells. The experiments were conducted both on CV-1 and COS-7 cells (CV-1 cells expressing the SV40 large T antigen) transiently expressing

HA; similar results were obtained in both cell lines. The cell surface HA proteins were labeled at 4°C by fluorescent Fab' fragments, and FRAP studies were conducted at 22°C. A typical curve of the lateral diffusion of Japan wt HA is shown in Fig. 2 A, and the average results of many such experiments are summarized in Fig. 3. As can be seen in Fig. 3, the lateral diffusion rate (measured by D, the lateral diffusion coefficient) of the nonraft mutant Japan HA-2A520 on cells under normal culture conditions was significantly higher (1.3–1.4-fold) than the rates measured for Japan wt HA, X:31 wt HA, and X:31 BHA-PI. The mobile fractions (R_f) of Japan wt HA and Japan HA-2A520 were high and similar; those of the HAs from the X:31 strain (BHA-PI and X:31 wt HA) were also similar to each other, although somewhat lower, most likely reflecting differences between the antibodies used to label the HAs from the different strains.

To further establish that the lower D of the DRM-associated HAs is due to interactions with lipid raft domains, we employed cholesterol depletion to disrupt cholesterol-sensitive

raft domains (Simons and Toomre, 2000). For all the HAs that associate with DRMs, this treatment significantly increased D to the level observed for Japan HA-2A520, which is not isolated in DRMs (Fig. 3). D of HA-2A520 was not affected by cholesterol depletion, in accord with the lack of association with rafts inferred from its sorting behavior and inability to partition into DRMs. We conclude that interactions with cholesterol-dependent lipid rafts retarded the lateral diffusion rate of the other three (DRM-associating) HA proteins.

Apical sorting of membrane proteins in polarized epithelial cells is proposed to depend on partitioning into Golgi or TGN raft-like domains. As some apical proteins (e.g., HA) can be isolated in DRMs only upon reaching the sorting point in the biosynthetic pathway (Skibbens et al., 1989) while other apical proteins are never isolated in DRMs, it has been argued that two separate and parallel pathways from the TGN to the apical surface may exist (Sarnataro et al., 2000; Jacob and Naim, 2001). Alternatively, the affinity for Golgi lipid rafts required for sorting an apical protein may be lower than that required for isolation in DRMs. To address the question of how measurements of detergent insolubility compare to measurements of raft association in living cells, we examined the behavior of two HA mutants differing by a single amino acid in the TM domain, TM 11.0 and TM 12.0 (Table I). Both the apical sorting of HA and its partitioning into Golgi DRMs depend upon its TM sequence (Skibbens et al., 1989; Scheiffele et al., 1997; Lin et al., 1998). Recently we have identified the minimum TM sequence required for apical sorting of HA and in the process produced several mutants including TM 11.0 that were sorted apically but were not isolated in DRMs (Alonso, M.A., personal communication; unpublished data). HA TM 11.0 was sorted less efficiently than TM 12.0, which does partition into DRMs (Table I), suggesting weaker association with rafts. The cholesterol-sensitive retardation of the lateral diffusion of HA mutants at the two extremes of raft association (raft-resident wt HA vs. the nonraft HA-2A520) correlated with their ability to enter DRMs (Scheiffele et al., 1997; Lin et al., 1998). To examine whether the correlation holds for weaker interactions, we used FRAP to investigate the interactions of TM 12.0 and TM 11.0 with cholesterol-sensitive rafts (Fig. 4). On untreated cells, D of TM 11.0 was significantly higher (1.5-fold) than that of TM 12.0. Importantly, cholesterol depletion increased D of TM 12.0 to the level observed for the non-DRM TM 11.0, whose lateral diffusion was insensitive to cholesterol depletion (Fig. 4). Thus, the in vivo FRAP studies are in accord with the detergent insolubility experiments (Table I) also for these mutants, suggesting that the strength of the interactions with rafts that can be detected by the two methods is similar. However, the apical sorting of HA TM 11.0 could still depend on raft interactions that are too weak for detection by both methods; this possibility has been validated by studies based on a combination of IgG-mediated patching and FRAP (see Fig. 8).

Immunofluorescence co-patching studies suggest transient interactions of DRM-associated HAs with raft domains

Lipid rafts were shown to be laterally mobile at the cell surface (Pralle et al., 2000). Therefore, the lower D of HAs that
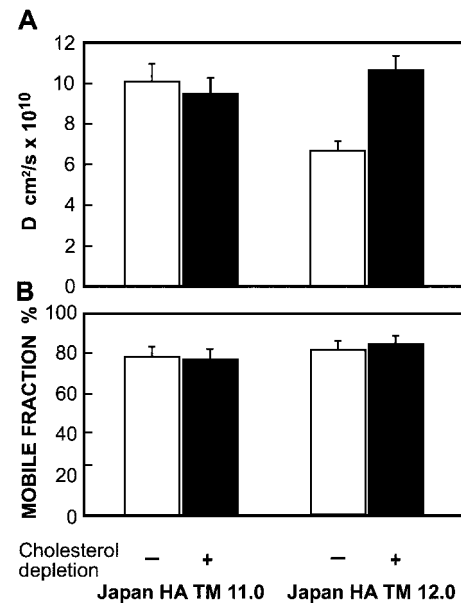

Figure 4. **Cholesterol-sensitive differences between the lateral diffusion rates of Japan HA TM 12.0 and Japan HA TM 11.0 mutants.** The experiments were performed as in Fig. 2, on COS-7 cells transiently transfected with the relevant SV40 expression vectors encoding each HA mutant (24 h after transfection). This period includes 18–20-h cholesterol depletion treatment where applicable. Each bar is the mean ± SEM of 30–40 measurements. (A) D values. D of TM 11.0 on untreated cells was significantly higher than D of TM 12.0 (P < 0.001). The increase in D of TM 12.0 after cholesterol depletion was also significant (P < 0.001), while D of TM 11.0 was not affected (P > 0.25). (B) Mobile fraction (R_f) values. The differences between R_f of the two mutants, with or without cholesterol depletion, were not significant (P > 0.20).

associate in vitro with DRMs relative to HAs excluded from DRMs could reflect stable association of a subpopulation of the DRM-associating HAs with rafts, yielding a slower average diffusion rate. Alternatively, the DRM-associating HAs may interact transiently with raft domains, in which case their diffusion would be retarded during the fraction of time they are associated with rafts. To differentiate between these possibilities, we employed immunofluorescence co-patching, as well as a combination of IgG-mediated patching and FRAP experiments (see next section).

Immunofluorescence studies based on antibody-mediated patching can identify putative raft association, if the association is stable enough to persist during patching (Mayor et al., 1994; Harder et al., 1998; Janes et al., 1999; Simons and Toomre, 2000). For coexpressed pairs of a GPI-anchored protein and HA, antibody-mediated patching was reported to bring together raft domains and cause their coalescence (Harder et al., 1998; Simons and Toomre, 2000). However, under the conditions used in those experiments, both vesicular stomatitis virus G protein and HA-Y543, proteins that are not isolated in DRMs, showed significant co-patching with the GPI-anchored placental alkaline phosphatase (Harder et al., 1998). We determined conditions that result in small distinct patches that increase the resolution for detecting co-patching and employed these in three sets of co-patching experiments (Fig. 5): (1) between two TM-anchored HA proteins, Japan wt HA and X:31 wt HA; (2)
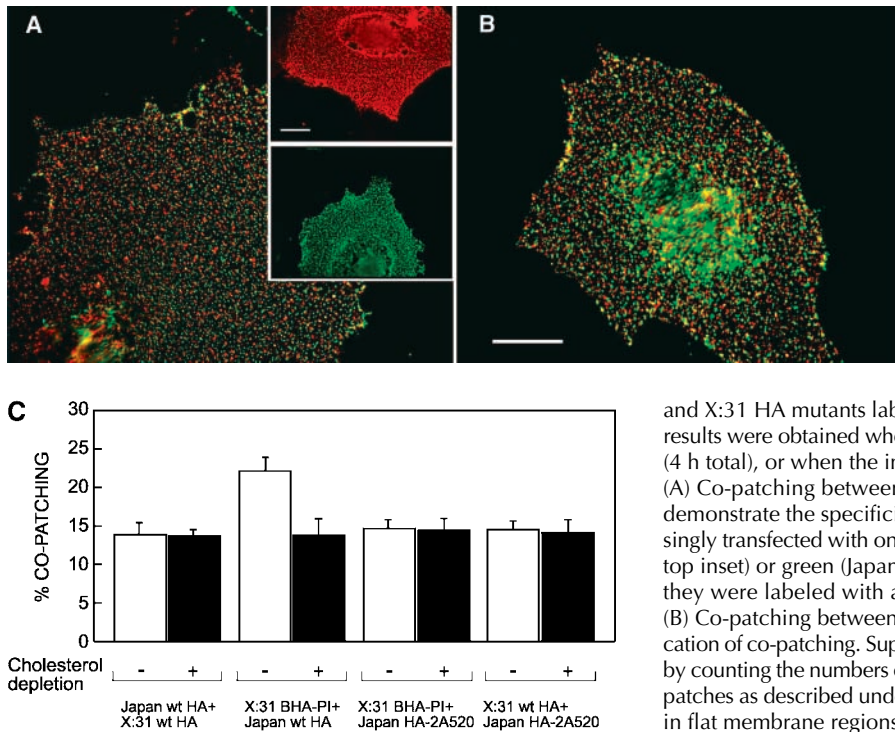
Figure 5. **Co-patching between pairs of Japan and X:31 HA mutants.** CV-1 cells were transfected transiently (see Materials and methods) by pairs of expression vectors encoding various HA mutants. Experiments were conducted 48 h after transfection. Where applicable, the cells were subjected to cholesterol depletion for the last 18–20 h after transfection. Live cells were consecutively labeled at 4°C by a series of antibodies (45 min each incubation) to mediate patching and fluorescent labeling (see Materials and methods), resulting in Japan HA mutants labeled by FITC (green) and X:31 HA mutants labeled by Alexa®594 (red). Bars, 20 μm. Similar results were obtained when the incubation periods were extended to 2 h (4 h total), or when the incubation temperature was increased to 18°C. (A) Co-patching between Japan wt HA and X:31 wt HA. The insets demonstrate the specificity of the labeling and patching protocol. Cells singly transfected with one HA type display exclusively red (X:31 wt HA, top inset) or green (Japan wt HA, bottom inset) fluorescence, although they were labeled with antibody mixtures for HAs from both strains. (B) Co-patching between X:31 BHA-PI and Japan wt HA. (C) Quantification of co-patching. Superimposed red and green images were analyzed by counting the numbers of green (G), red (R), and overlapping (yellow, Y) patches as described under the Materials and methods, counting patches in flat membrane regions (10×10 μm^2) on 20–25 cells in each case. The percent co-patching (% of one protein in mutual patches with the coexpressed HA protein) is given by $100 \times (Y/[Y + G])$ and by $100 \times (Y/[Y + R])$ for the green- and red-labeled HAs, respectively. As the results were similar (within 2%) for green and red labeling, the average value is shown for each pair. The bars are mean ± SEM. Except for the pair X:31 BHA-PI/Japan wt HA, the co-patching levels of the various pairs on untreated cells were not significantly different from the control pairs of X:31 wt HA or X:31 BHA-PI with Japan HA-2A520 ($P > 0.25$). The % co-patching of BHA-PI/Japan wt HA was significantly higher ($P < 0.001$) and was significantly reduced by cholesterol depletion ($P < 0.001$).

between Japan wt HA and GPI-anchored X:31 BHA-PI; and (3) between X:31 wt HA or BHA-PI and the nonraft mutant Japan HA-2A520 as controls. In the co-patching method (detailed in Keren et al., 2001), two antigenically distinct membrane proteins are coexpressed at the surface of live cells. One is forced into micropatches (in the cold, to avoid endocytosis) by a double layer of bivalent IgGs, using a fluorescent secondary IgG. The coexpressed protein is patched/labeled by IgG from another species and a secondary IgG coupled to another fluorophore. If the two proteins reside in mutual clusters or domains and do not dissociate from them appreciably during patching, they are swept into mutual patches. Using secondary IgGs coupled to red and green fluorophores, mutual patches appear yellow when the two images are overlapped. This holds also when the proteins are oligomeric; for this matter, a trimeric HA is a single unit, and one measures the association between several such units in clusters/domains. As HA is trimeric, studies on its clustering require coexpression of two antigenically distinct HAs that form only separate trimers. This condition is met by the HAs of the Japan and X:31 strains (Boulay et al., 1988; Keren et al., 2001). Typical co-patching results are shown in Fig. 5 (A and B); the averaged results of many such experiments are depicted in Fig. 5 C. The co-patching between Japan and X:31 wt HA proteins was very low (14%) and was not affected by cholesterol depletion. This low value is similar to that measured between the various HAs and the nonraft mutant HA-2A520 (Fig. 5 C), suggesting that this background co-patching level is not due to residual localization in

rafts. It most likely represents the cumulative contribution of factors other than coresidence in rafts (e.g., occasional overlap of randomly distributed green and red patches, mutual targeting to other cellular structures, or nonspecific interactions). Interestingly, the pair of X:31 BHA-PI/Japan wt HA exhibited a small but significant cholesterol-sensitive increase in the co-patching level (Fig. 5 C). The low levels of co-patching between pairs of raft-associated HAs suggest that at least one HA in a coexpressed pair interacts transiently with the raft domains, enabling its dissociation during the patching step. The higher level of co-patching between BHA-PI and wt HA is in accord with the proposal that antibody cross-linking of GPI-anchored proteins stabilizes the raft domains (Harder et al., 1998; Simons and Toomre, 2000).

FRAP studies reveal differences between the interaction dynamics of wt HA and BHA-PI with raft patches and demonstrate raft association for TM 11.0

To further explore the dynamics of HA–raft interactions, we coexpressed pairs of HA proteins (X:31 BHA-PI with either Japan wt HA or Japan HA-2A520) in CV-1 or COS-7 cells. One protein (e.g., X:31 BHA-PI) was cross-linked by double labeling with IgGs as in the patching experiments. The coexpressed HA (e.g., Japan wt HA) was labeled by monovalent Fab' tagged with another fluorophore, and its lateral diffusion was measured by FRAP. Typical curves are shown in Fig. 6, and the averaged data are summarized in Fig. 7. The IgG-mediated patching led to lateral immobilization of the cross-linked HA protein (Fig. 6 A). Immobilization of X:31

Figure 6. **Representative FRAP curves measuring the effects of immobilizing one HA protein on the lateral diffusion of another.** Cells were cotransfected with pairs of antigenically distinct HA proteins. After 48 h (CV-1 cells) or 24 h (COS-7 cells), one type of HA was cross-linked by IgGs (30 μg/ml HC3 mouse α-X:31 HA or Fc125 mouse α-Japan HA, followed by 30 μg/ml GαM FITC-IgG), while the coexpressed HA type was labeled by monovalent Fab' (100 μg/ml α-Japan rabbit TRITC-Fab', or 50 μg/ml α-X:31 rabbit Fab' followed by 50 μg/ml GαR TRITC-Fab'). FRAP experiments were conducted at 22°C as in Fig. 2, identifying coexpressing cells by their FITC fluorescence. (A) Lateral diffusion of IgG–cross-linked X:31 BHA-PI. Only the R_f value is shown, as the recovery was too low to allow determination of D. Similar immobilization was measured for IgG–cross-linked Japan wt HA or Japan HA-2A520. (B) Lateral diffusion of Japan wt HA in the presence of IgG–cross-linked X:31 BHA-PI. (C) Effect of cross-linking Japan wt HA on the lateral diffusion of X:31 BHA-PI. (D) Lack of effect of cross-linking X:31 BHA-PI on the lateral diffusion of Japan HA-2A520.
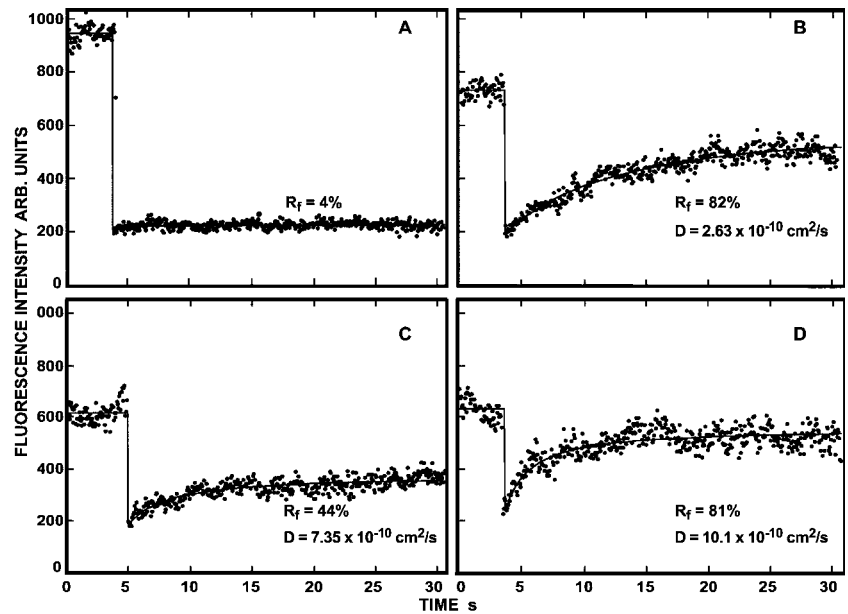

BHA-PI mediated a significant reduction (twofold) in D of the coexpressed Japan wt HA, without affecting its R_f (Fig. 6 B and Fig. 7). The effect required patching/immobilization of the coexpressed X:31 BHA-PI (Fig. 7 A) and was not detected when the nonraft Japan HA-2A520 mutant was coexpressed with X:31 BHA-PI (Fig. 6 D and Fig. 7). A reduction in D with no change in R_f is typical of transient interactions with immobile domains (in this case, patches of domains containing BHA-PI), as explained by us earlier (Fire et al., 1991, 1995). This occurs because each molecule of coexpressed Japan wt HA will undergo several association/dissociation cycles with the immobile patches during the FRAP measurements, spending some of the time bound to the immobile entity while being free to diffuse during the dissociation cycle. On the other hand, stable association for the entire FRAP measurement (30 s) would reduce R_f with no effect on D, because a molecule associated with the immobile entity remains bound for the entire duration of the measurement. Such an opposite effect (reduction in R_f with no effect on D) was measured for the lateral diffusion of X:31 BHA-PI when coexpressed Japan wt HA was patched and immobilized using IgGs (Fig. 6 C and Fig. 7); the specificity is demonstrated by the lack of such effects on X:31 BHA-PI mobility after patching of coexpressed Japan HA-2A520 (Fig. 7, C and D). The stable association is observed not only for BHA-PI, but also for other GPI-anchored proteins. Thus, GFP-GPI (GFP fused to the GPI anchor of the folate receptor) behaved similar to BHA-PI in patching/FRAP studies; immobilization of coexpressed wt HA reduced R_f of GFP-GPI (from 96 ± 2% to 60 ± 4%, $n = 25$, P < 0.001) without affecting its D value ([2.8 ± 0.5] × 10^{-8} cm^2/s in both cases), while immobilization of GFP-GPI using mouse anti-GFP and secondary goat anti–mouse IgG had no effect on R_f of Japan wt HA, but reduced its D value (from [7.7 ± 0.4] × 10^{-10} to [4.3 ± 0.5] × 10^{-10} cm^2/s, $n = 25$, P < 0.001). Our results suggest that the GPI-anchored BHA-PI (or GFP-GPI) and wt HA can reside

in mutual rafts, but their mode of interaction with the raft domains, at least after IgG-mediated patching, is different (stable association for GPI-anchored proteins vs. transient interaction for wt HA).

The sensitivity of the combined patching/FRAP experiments for detecting interactions with rafts is higher, because the mobility of the coexpressed protein that is not cross-linked is now inhibited by interactions with immobile raft
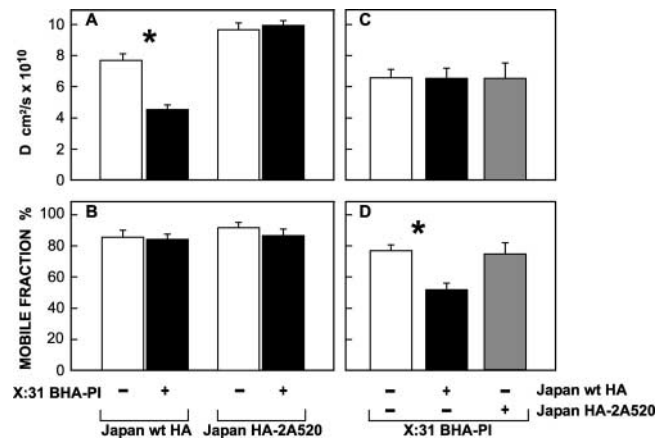
Figure 7. **Cross-linking of one HA in a pair of coexpressed HA proteins has differential effects on the lateral diffusion of wt HA and BHA-PI.** Experiments were performed as in Fig. 6. Bars are mean ± SEM of 20–30 measurements. Asterisks indicate significant differences from the uncross-linked control (P < 0.001, t test). (A and B) Lateral diffusion of Japan wt HA and Japan HA-2A520 in the presence (+) or absence (−) of coexpressed, IgG–cross-linked X:31 BHA-PI. Control experiments in which coexpressed X:31 BHA-PI was labeled with FITC-Fab' to avoid cross-linking and immobilization yielded results similar to the (−) control. (C and D) Lateral diffusion of X:31 BHA-PI in the presence (+) or absence (−) of coexpressed, IgG–cross-linked Japan wt HA or Japan HA-2A520. Labeling the coexpressed Japan HAs with FITC-Fab' to avoid cross-linking and immobilization yielded results similar to singly expressed BHA-PI.
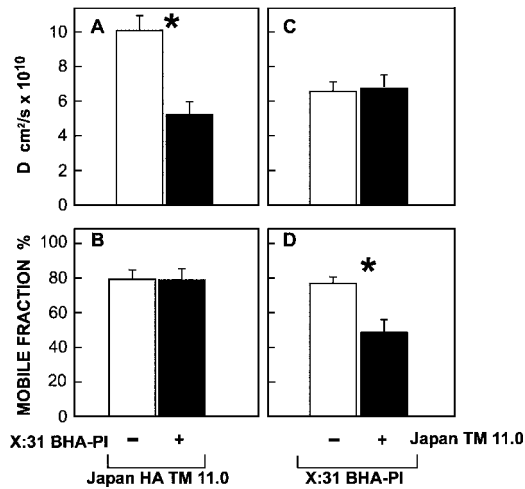
Figure 8. **Cross-linking/FRAP studies demonstrate transient association of HA TM 11.0 with rafts.** Experiments were conducted as in Fig. 7. Bars are mean ± SEM of 25 measurements. Significant differences (P < 0.001) are indicated by asterisks. (A and B) Lateral diffusion of Japan HA TM 11.0 with (+) or without (−) IgG–cross-linked X:31 BHA-PI. (C and D) Lateral diffusion of X:31 BHA-PI in the presence (+) or absence (−) of IgG–cross-linked Japan HA TM 11.0.

aggregates (as opposed to laterally mobile small rafts in the absence of cross-linking). We therefore applied this approach to explore whether it can detect raft association of the HA mutant TM 11.0, which can undergo apical sorting but is not isolated in vitro in DRMs. The results (Fig. 8) show a reduction in D of HA TM 11.0 after IgG-mediated immobilization of BHA-PI, and a reduction in R_f (but not D) of BHA-PI upon immobilization of TM 11.0. This demonstrates that HA TM 11.0 interacts transiently with mutual rafts containing BHA-PI.

Discussion

Many biological functions are attributed to lipid rafts (Kurzchalia and Parton, 1999; Brown and London, 2000; Simons and Toomre, 2000; Anderson and Jacobson, 2002), but the details of how rafts might function are still unknown. Thus, it is not clear whether proteins targeted to rafts by different signals share the same rafts, and whether their association with raft domains is stable or transient. Our studies demonstrate that association of HA proteins with lipid rafts reduces their lateral diffusion rate and that this inhibition is released after cholesterol depletion, enabling the measurement of association with rafts in live cells. By combining IgG cross-linking and FRAP, we find that HA proteins with different raft-targeting signals (a GPI anchor vs. specific TM sequences) can share the same raft domains, but the dynamics of their interactions with rafts are different (stable association for GPI-anchored proteins vs. transient interactions for the TM-directed HA). Our results indicate that this method can measure in vivo interactions with raft patches that are too weak to be detected in vitro by detergent insolubility, and that these weaker interactions may suffice for some biological functions, such as apical sorting in epithelial cells.

In the current study, we combined FRAP and co-patching studies to investigate these issues in live cells expressing a se-

ries of HA mutants that differ in their ability to be isolated in DRMs and to undergo apical sorting. The HA cytoplasmic tail is short and lacks signals known to interact with intracellular structures (Lazarovits and Roth, 1988; Kusumi and Sako, 1996), providing an experimental system that is not complicated by possible interactions with the cytoskeleton. Furthermore, the availability of HA mutants that vary in DRM affinity enables a direct comparison between the effects of mutations introduced into the same protein background. Our results (Figs. 2 and 3) demonstrate that the lateral diffusion rates of DRM-associating HA proteins (X:31 BHA-PI and wt HA) are significantly slower than that of an HA mutant (HA-2A520) that is excluded from DRMs and not sorted apically. This suggests that the lateral diffusion of the DRM-associating HAs is retarded by interactions with lipid rafts, a conclusion supported by the selective effects of cholesterol depletion on the HA proteins. Only D of DRM-associating HA proteins was elevated, reaching the same values measured for HA-2A520, whose mobility is insensitive to cholesterol (Fig. 3). As no IgG cross-linking is applied here, these results suggest that the raft domains with which wt HA and BHA-PI interact exist prior to IgG cross-linking. Our findings are in line with a study by single particle tracking (Pralle et al., 2000), which showed a cholesterol-sensitive increase in viscous drag (equivalent to a reduction in D) for some DRM-resident proteins. This retardation was about twofold higher than in our measurements of raft-resident HA proteins, probably reflecting the average nature of FRAP studies, where HA populations in and out of rafts both contribute to the measurements. Another possibility (not mutually exclusive) is that the association of some HA proteins with rafts may be transient, in which case their lateral diffusion would be retarded only during the association cycle, resulting in an apparent D value between that of a raft and of a nonraft HA protein.

The measurements of the association of HA mutants with raft domains by the sensitivity of their lateral diffusion to cholesterol depletion (Fig. 3) are in good agreement with their detergent insolubility (Scheiffele et al., 1997; Lin et al., 1998; Fig. 1 and Table I), suggesting comparable sensitivities of the two methods. However, the Triton X-100–insoluble fraction of BHA-PI was less than that of wt HA (unpublished data), although BHA-PI exhibited stable interaction with rafts in FRAP co-patching experiments while wt HA displayed transient interactions. This suggests that the fraction of BHA-PI in rafts is not higher than that of wt HA. Yet, BHA-PI dissociation from raft patches is much slower (Figs. 6 and 7), raising the possibility that the dissociation rate of a protein from raft domains does not necessarily correlate with the equilibrium constant.

Interestingly, both detergent insolubility (Table I) and FRAP studies (Fig. 4) failed to detect interactions of HA TM 11.0 with lipid rafts, although this HA mutant still undergoes significant apical sorting (Alonso, M.A., personal communication; unpublished data). Because the apical sorting of HA proteins depends critically on partitioning into Golgi raft domains (Skibbens et al., 1989; Scheiffele et al., 1997; Lin et al., 1998; Melkonian et al., 1999), this finding suggests that the affinity to Golgi raft domains required for apical sorting may be weaker than that required to produce

interactions that are measurable by the commonly employed methods (e.g., in vitro isolation in DRMs). This conclusion is strongly supported by the demonstration (Fig. 8) that the more sensitive method based on combining IgG-mediated patching and FRAP (see next paragraph) was capable of detecting association of HA TM 11.0 with rafts.

To investigate the dynamics of HA–raft interactions, we employed immunofluorescence co-patching in combination with FRAP. A former study examined co-patching between a GPI-anchored protein and HA, but not between two different proteins targeted to rafts by their TM regions (such as two antigenically distinct wt HA proteins), and was also complicated by the detection of co-patching with nonraft TM proteins (Harder et al., 1998). We improved the resolution by defining conditions that lead to small and distinct patches and examined both the co-patching of GPI-anchored HA with wt HA and of one wt HA with another (Japan wt HA with X:31 wt HA). An important control is provided by the very low co-patching level obtained between X:31 wt HA and the nonraft mutant HA-2A520 (Fig. 5). A similar low co-patching level was measured for the pair of Japan wt HA/X:31 wt HA, suggesting either that they reside in separate rafts or that they interact transiently with raft domains and dissociate from them during the patching step. A significantly higher level of co-patching was found only when GPI-anchored HA was co-patched with wt HA, and this higher level was sensitive to cholesterol depletion (Fig. 5). This is in line with the suggestion that antibody-mediated aggregation of GPI-anchored proteins can stabilize and mediate coalescence of raft domains (Harder et al., 1998; Simons and Toomre, 2000). However, even in this case, the level of co-patching is not very high (22–23%, on a background level of 14%), suggesting that although IgG cross-linking stabilizes to some extent the association with rafts, at least one of the two HA proteins examined can still dissociate from rafts to some degree during patching. As shown by the combined IgG patching/FRAP studies (Figs. 6 and 7), this protein is the transiently interacting wt HA.

Due to the weak (logarithmic) dependence of the lateral diffusion rate of membrane proteins on size (Saffman and Delbruck, 1975), raft domains may diffuse only somewhat slower than a nonraft membrane protein (Pralle et al., 2000). This makes it difficult to distinguish between a protein with a subpopulation that diffuses slower while stably associated with rafts, and a protein whose diffusion is retarded due to transient interactions with rafts. Therefore, we employed IgG cross-linking to immobilize one HA protein and measured by FRAP the effects on the lateral diffusion of a coexpressed HA mutant labeled with Fab'. Stable association of a protein with the immobilized patches of a coexpressed protein reduces its mobile fraction (R_f), while transient interactions reduce its lateral diffusion rate (D). If the two proteins do not interact or do not share the same raft domains, immobilization of one should not affect either R_f or D of the other. The results of this series of experiments (Figs. 6–8) lead to several important conclusions. First, the finding that patching/immobilization of BHA-PI, GFP-GPI, or wt HA does affect the lateral diffusion of the coexpressed protein demonstrates the coexistence of the two proteins in the same rafts. Second, the reduction in D of wt HA

upon immobilization of BHA-PI (or GFP-GPI) suggests that wt HA interacts transiently with raft domains containing the GPI-anchored protein, even when the latter have been cross-linked by IgGs. Third, the reduction in R_f of BHA-PI (or GFP-GPI) upon immobilization of coexpressed wt HA indicates that the GPI-anchored proteins are stably associated with rafts containing IgG–cross-linked wt HA. Thus, the same raft domains can exhibit stable association with some proteins and transient interactions with others. The identification of both types of interactions has implications for potential models of rafts as scaffolds that regulate biological functions. Some models would require stable association with rafts, e.g., activation by dimerization/oligomerization of two proteins already concentrated in the same raft, or activation of two proteins in different rafts by clustering the rafts together, allowing their coalescence (Kurzchalia and Parton, 1999; Brown and London, 2000; Simons and Toomre, 2000). Other models may require transient association with rafts to allow dynamic exchange into and out of these domains. Such is the case for activation due to altered partitioning of specific proteins in the raft domains after ligand binding and/or dimerization (Simons and Toomre, 2000). Another example is signaling by H-Ras, proposed to occur in two steps: activation of H-Ras within rafts, followed by its obligatory exit from the raft domains (Prior et al., 2001). Obviously, this would require the interactions of H-Ras with rafts to be transient. Our demonstration that different raft-associated proteins can display either stable or transient interactions with mutual raft domains suggests that both possibilities exist. The dynamics of the association with rafts may depend on the raft-targeting signal of the specific protein, as different moieties (e.g., a GPI anchor vs. a TM sequence) can interact differently with lipid and/or protein constituents of rafts.

Materials and methods

Materials
CV-1 and COS-7 cells (American Type Culture Collection) were maintained in DME with 10% FCS (Biological Industries Beth Haemek or Life Technologies) as previously described (Keren et al., 2001). Proteins were labeled with EXPRE[^{35}S][^{35}S] protein labeling mix (PerkinElmer). Rabbit polyclonal IgG against Japan HA (α-Japan) has been previously described (Fire et al., 1991, 1995). Rabbit anti–X:31 HA IgG (α-X:31) was provided by J.M. White (University of Virginia, Charlottesville, VA). Preparation of monovalent Fab' from rabbit IgGs and tagging with TRITC (Molecular Probes) followed standard procedures (Fire et al., 1991). HC3 mouse monoclonal α-X:31 HA (Daniels et al., 1983) was a gift from J.J. Skehel (National Institute for Medical Research, London, UK), and Fc125 mouse monoclonal α-Japan HA (Braciale et al., 1981) was a gift from T.J. Braciale (University of Virginia, Charlottesville, VA). Mouse anti-GFP was from StressGen Biotechnologies. Goat anti–rabbit (GαR) IgG coupled to Alexa®594 (GαR Alexa 594-IgG) was from Molecular Probes. Goat anti–mouse (GαM) IgG coupled to FITC (GαM FITC-IgG) and normal goat IgG were from Jackson ImmunoResearch Laboratories. Monovalent GαR TRITC-Fab' was prepared from TRITC-tagged F(ab')$_2$ fragments of GαR IgG (Jackson ImmunoResearch Laboratories) (Fire et al., 1991).

Plasmids and recombinant virus vectors
The studies used several expression vectors (pkSVE for infection with recombinant SV40 viruses, all other vectors for transient transfection) encoding HA proteins. X:31 HA (Gething et al., 1980) in pkSVE (Keren et al., 2001) was also subcloned into pCB4 (Brewer, 1994). BHA-PI (the TM and cytoplasmic domains of X:31 HA replaced by nine amino acids from the GPI anchor addition signal of DAF, with a serine-for-lysine substitution) (Kemble et al., 1994) in the pEE14 vector (Celltech) was a gift from J.M.

White. Expression plasmid for GFP-GPI (EGFP attached to the folate receptor GPI anchor signal) (Sabharanjak et al., 2002) was a gift from R.G. Parton (University of Queensland, Brisbane, Australia). Several mutants derived from the cDNA encoding A/Japan/305/57 HA were used (Lin et al., 1998; Table I). These cDNAs were introduced into the SV40-based vector pkSVE and also subcloned into transient expression vectors (pSVT7 for Japan wt HA; pCB6 for HA-2A520, TM 12.0, and TM 11.0).

Cell transfection and infection
CV-1 cells were infected with recombinant SV40 virus vectors; alternatively, COS-7 or CV-1 cells were subjected to direct transfection using Fugene 6 (Roche Chemicals). Infection of CV-1 cells was carried out as previously described (Naim and Roth, 1994), using second or third passage recombinant SV40 virus stocks prepared from the HA mutants cloned in pkSVE vectors. The infected cells were plated on glass coverslips for immunofluorescence-based studies. Experiments were conducted 36–38 h after infection. Direct transfection using HAs cloned in expression vectors containing SV40 origin (pSVT7, pCB6, pEE14, and pEGFP) was carried out with Fugene 6 on subconfluent cells grown on glass coverslips. They were taken for co-patching or FRAP studies either after 48 h (CV-1 cells) or 24 h (the higher-expressing COS-7 cells).

Cholesterol depletion
After transfection or infection with HA-expressing vectors, the cells were preincubated at 37°C for 4–6 h (transfected COS-7 cells), 16–18 h (infected CV-1 cells), or 28–30 h (transfected CV-1 cells), and subjected to cholesterol depletion by incubation (18–20 h) with 50 μM compactin and 50 μM mevalonate in DME supplemented with 10% lipoprotein-deficient serum following established procedures (Hua et al., 1996; Lin et al., 1998).

Triton X-100 insolubility
COS-7 cells (1.25×10^5) were replated from a subconfluent plate and transfected with expression plasmids for wt Japan HA or HA-2A520. After 24 h, cholesterol was depleted from the cells for 24 h as described in the previous section. The cells were washed four times in PBS plus 1 mM MgCl$_2$ and 0.1 mM CaCl$_2$, and incubated in DME lacking methionine and cysteine for 30 min at 37°C. The cells were radiolabeled with EXPRE[^{35}S][^{35}S] protein labeling mix at a concentration of 0.5 mCi/ml for 30 min at 37°C, followed by a chase in DME for 100 min at 37°C. Samples were lysed on ice in 1% Triton X-100 buffer, and soluble and insoluble fractions were prepared, immunoprecipitated, and analyzed by PAGE as previously described (Lin et al., 1998).

Immunofluorescence co-patching
Antibody-mediated co-patching (Gilboa et al., 2000) of antigenically distinct HA mutants was measured as previously described (Keren et al., 2001). In brief, CV-1 or COS-7 cells were infected or transfected with pairs of vectors encoding X:31 and Japan HA proteins, and subjected in some experiments to cholesterol depletion. All further incubations (at 4°C, to allow only cell surface labeling and eliminate internalization) were in HBSS supplemented with 20 mM Hepes, pH 7.2, and 1% BSA (HBSS/Hepes/BSA). The cells were incubated successively with the following IgGs (30 μg/ml, 45 min): (1) Fc125 mouse α-Japan and rabbit α-X:31, together with 200 μg/ml normal goat IgG for blocking; and (2) GαR Alexa®594-IgG and GαM FITC-IgG. The cells were fixed as previously described (Harder et al., 1998) and mounted with Prolong Antifade (Molecular Probes). Images were recorded with a CCD camera as previously described (Gilboa et al., 2000). Superposition of the green and red channels and determination of the numbers of red, green, and overlapping (yellow) patches were performed using Image-Pro Plus software (Media Cybernetics), defining pairs of green/red patches as overlapping if the peaks of intensity of two nearest-neighbor patches were separated by <0.2 μm.

FRAP
FRAP studies were conducted on cells singly or doubly transfected with HA expression vectors exactly as described for co-patching. HA proteins at the cell surface were labeled with TRITC-tagged monovalent Fab′ fragments, either alone or together with cross-linking IgGs against the antigenically distinct coexpressed HA protein (for details, see figure legends). Lateral diffusion coefficients (D) and mobile fractions were measured by FRAP (Axelrod et al., 1976; Koppel et al., 1976) using previously described instrumentation (Fire et al., 1991). The experiments were conducted at 22°C in HBSS/Hepes/BSA. The monitoring argon ion laser beam (529.5 nm, 1 μW) was focused through the microscope (Carl Zeiss MicroImaging, Inc.) to a Gaussian radius of 0.85 ± 0.02 μm (63× oil immersion objective). A brief pulse (5 mW, 10–15 ms) bleached 50–70% of the fluores-

cence in the illuminated region. Fluorescence recovery was followed by the attenuated monitoring beam. D and R_f were determined by nonlinear regression analysis, fitting to the lateral diffusion equation of a single species (single D value) (Fire et al., 1995).

References

Anderson, R.G., and K. Jacobson. 2002. A role for lipid shells in targeting proteins to caveolae, rafts, and other lipid domains. *Science.* 296:1821–1825.

Axelrod, D., D.E. Koppel, J. Schlessinger, E.L. Elson, and W.W. Webb. 1976. Mobility measurement by analysis of fluorescence photobleaching recovery kinetics. *Biophys. J.* 16:1055–1069.

Boulay, F., R.W. Doms, R.G. Webster, and A. Helenius. 1988. Posttranslational oligomerization and cooperative acid activation of mixed influenza hemagglutinin trimers. *J. Cell Biol.* 106:629–639.

Braciale, T.J., M.E. Andrew, and V.L. Braciale. 1981. Simultaneous expression of H-2-restricted and alloreactive recognition by a cloned line of influenza virus-specific cytotoxic T lymphocytes. *J. Exp. Med.* 153:1371–1376.

Brewer, C.B. 1994. Cytomegalovirus plasmid vectors for permanent lines of polarized epithelial cells. *Methods Cell Biol.* 43:233–245.

Brown, D.A., and E. London. 2000. Structure and function of sphingolipid- and cholesterol-rich membrane rafts. *J. Biol. Chem.* 275:17221–17224.

Daniels, R.S., A.R. Douglas, J.J. Skehel, and D.C. Wiley. 1983. Analyses of the antigenicity of influenza haemagglutinin at the pH optimum for virus-mediated membrane fusion. *J. Gen. Virol.* 64:1657–1662.

Ehehalt, R., P. Keller, C. Haass, C. Thiele, and K. Simons. 2003. Amyloidogenic processing of the Alzheimer β-amyloid precursor protein depends on lipid rafts. *J. Cell Biol.* 160:113–123.

Fire, E., D.E. Zwart, M.G. Roth, and Y.I. Henis. 1991. Evidence from lateral mobility studies for dynamic interactions of a mutant influenza hemagglutinin with coated pits. *J. Cell Biol.* 115:1585–1594.

Fire, E., O. Gutman, M.G. Roth, and Y.I. Henis. 1995. Dynamic or stable interactions of influenza hemagglutinin mutants with coated pits: dependence on the internalization signal but not on aggregation. *J. Biol. Chem.* 270:21075–21081.

Friedrichson, T., and T.V. Kurzchalia. 1998. Microdomains of GPI-anchored proteins in living cells revealed by crosslinking. *Nature.* 394:802–805.

Gething, M.J., J. Bye, J. Skehel, and M. Waterfield. 1980. Cloning and DNA sequence of double-stranded copies of haemagglutinin genes from H2 and H3 strains elucidates antigenic shift and drift in human influenza virus. *Nature.* 287:301–306.

Gilboa, L., A. Nohe, T. Geissendorfer, W. Sebald, Y.I. Henis, and P. Knaus. 2000. Bone morphogenetic protein receptor complexes on the surface of live cells: a new oligomerization mode for Serine/Threonine kinase receptors. *Mol. Biol. Cell.* 11:1023–1035.

Grakoui, A., S.K. Bromley, C. Sumen, M.M. Davis, A.S. Shaw, P.M. Allen, and M.L. Dustin. 1999. The immunological synapse: a molecular machine controlling T cell activation. *Science.* 285:221–227.

Harder, T., P. Scheiffele, P. Verkade, and K. Simons. 1998. Lipid domain structure of the plasma membrane revealed by patching of membrane components. *J. Cell Biol.* 141:929–942.

Hua, X., J. Sakai, M.S. Brown, and J.L. Goldstein. 1996. Regulated cleavage of sterol regulatory element binding proteins requires sequences on both sides of the endoplasmic reticulum membrane. *J. Biol. Chem.* 271:10379–10384.

Jacob, R., and H.Y. Naim. 2001. Apical membrane proteins are transported in distinct vesicular carriers. *Curr. Biol.* 11:1444–1450.

Janes, P.W., S.C. Ley, and A.I. Magee. 1999. Aggregation of lipid rafts accompanies signaling via the T cell antigen receptor. *J. Cell Biol.* 147:447–461.

Kemble, G.W., T. Danieli, and J.M. White. 1994. Lipid-anchored influenza hemagglutinin promotes hemifusion, not complete fusion. *Cell.* 76:383–391.

Kenworthy, A.K., and M. Edidin. 1998. Distribution of a glycosylphosphatidylinositol-anchored protein at the apical surface of MDCK cells examined at a resolution of <100 A using imaging fluorescence resonance energy transfer. *J. Cell Biol.* 142:69–84.

Kenworthy, A.K., N. Petranova, and M. Edidin. 2000. High-resolution FRET microscopy of cholera toxin B-subunit and GPI-anchored proteins in cell plasma membranes. *Mol. Biol. Cell.* 11:1645–1655.

Keren, T., M.G. Roth, and Y.I. Henis. 2001. Internalization-competent influenza hemagglutinin mutants form complexes with clathrin-deficient multivalent AP-2 oligomers in live cells. *J. Biol. Chem.* 276:28356–28363.

Koppel, D.E., D. Axelrod, J. Schlessinger, E.L. Elson, and W.W. Webb. 1976. Dynamics of fluorescence marker concentration as a probe of mobility. *Biophys. J.* 16:1315–1329.

Kurzchalia, T.V., P. Dupree, R.G. Parton, R. Kellner, H. Virta, M. Lehnert, and K. Simons. 1992. VIP21, a 21-kD membrane protein is an integral component of trans Golgi network–derived transport vesicles. *J. Cell Biol.* 118:1003–1014.

Kurzchalia, T.V., and R.G. Parton. 1999. Membrane microdomains and caveolae. *Curr. Opin. Cell Biol.* 11:424–431.

Kusumi, A., and Y. Sako. 1996. Cell surface organization by the membrane skeleton. *Curr. Opin. Cell Biol.* 8:566–574.

Lazarovits, J., and M.G. Roth. 1988. A single amino acid change in the cytoplasmic domain allows the influenza virus hemagglutinin to be endocytosed through coated pits. *Cell.* 53:743–752.

Lin, S., H.Y. Naim, A.C. Rodriguez, and M.G. Roth. 1998. Mutations in the middle of the transmembrane domain reverse the polarity of transport of the influenza virus hemagglutinin in MDCK epithelial cells. *J. Cell Biol.* 142:51–57.

Mayor, S., K.G. Rothberg, and F.R. Maxfield. 1994. Sequestration of GPI-anchored proteins in caveolae triggered by cross-linking. *Science.* 264:1948–1951.

Melkonian, K.A., A.G. Ostermeyer, J.Z. Chen, M.G. Roth, and D.A. Brown. 1999. Role of lipid modifications in targeting proteins to detergent-resistant membrane rafts. Many raft proteins are acylated, while few are prenylated. *J. Biol. Chem.* 274:3910–3917.

Naim, H.Y., and M.G. Roth. 1994. Characteristics of the internalization signal in the Y543 influenza virus hemagglutinin suggest a model for recognition of internalization signals containing tyrosine. *J. Biol. Chem.* 269:3928–3933.

Pralle, A., P. Keller, E. Florin, K. Simons, and J.K. Horber. 2000. Sphingolipid-cholesterol rafts diffuse as small entities in the plasma membrane of mammalian cells. *J. Cell Biol.* 148:997–1008.

Prior, I.A., A. Harding, J. Yan, J. Sluimer, R.G. Parton, and J.F. Hancock. 2001. GTP-dependent segregation of H-ras from lipid rafts is required for biological activity. *Nat. Cell Biol.* 3:368–375.

Prusiner, S.B. 1998. Prions. *Proc. Natl. Acad. Sci. USA.* 95:13363–13383.

Roper, K., D. Corbeil, and W.B. Huttner. 2000. Retention of prominin in microvilli reveals distinct cholesterol-based lipid micro-domains in the apical plasma membrane. *Nat. Cell Biol.* 2:582–592.

Rothberg, K.G., J.E. Heuser, W.C. Donzell, Y.S. Ying, J.R. Glenney, and R.G. Anderson. 1992. Caveolin, a protein component of caveolae membrane coats. *Cell.* 68:673–682.

Sabharanjak, S., P. Sharma, R.G. Parton, and S. Mayor. 2002. GPI-anchored proteins are delivered to recycling endosomes via a distinct cdc42-regulated, clathrin-independent pinocytic pathway. *Dev. Cell.* 2:411–423.

Saffman, P.G., and M. Delbruck. 1975. Brownian motion in biological membranes. *Proc. Natl. Acad. Sci. USA.* 72:3111–3113.

Sarnataro, D., L. Nitsch, W. Hunziker, and C. Zurzolo. 2000. Detergent insoluble microdomains are not involved in transcytosis of polymeric Ig receptor in FRT and MDCK cells. *Traffic.* 1:794–802.

Scheiffele, P., M.G. Roth, and K. Simons. 1997. Interaction of influenza virus haemagglutinin with sphingolipid-cholesterol membrane domains via its transmembrane domain. *EMBO J.* 16:5501–5508.

Simons, K., and E. Ikonen. 1997. Functional rafts in cell membranes. *Nature.* 387:569–572.

Simons, K., and D. Toomre. 2000. Lipid rafts and signal transduction. *Nat. Rev. Mol. Cell Biol.* 1:31–39.

Skibbens, J.E., M.G. Roth, and K.S. Matlin. 1989. Differential extractability of influenza virus hemagglutinin during intracellular transport in polarized epithelial cells and nonpolar fibroblasts. *J. Cell Biol.* 108:821–832.

Smart, E.J., G.A. Graf, M.A. McNiven, W.C. Sessa, J.A. Engelman, P.E. Scherer, T. Okamoto, and M.P. Lisanti. 1999. Caveolins, liquid-ordered domains, and signal transduction. *Mol. Cell. Biol.* 19:7289–7304.

Tanimura, N., M. Nagafuku, Y. Minaki, Y. Umeda, F. Hayashi, J. Sakakura, A. Kato, D.R. Liddicoat, M. Ogata, T. Hamaoka, and A. Kosugi. 2003. Dynamic changes in the mobility of LAT in aggregated lipid rafts upon T cell activation. *J. Cell Biol.* 160:125–135.

Thomsen, P., K. Roepstorff, M. Stahlhut, and B. van Deurs. 2002. Caveolae are highly immobile plasma membrane microdomains, which are not involved in constitutive endocytic trafficking. *Mol. Biol. Cell.* 13:238–250.

Varma, R., and S. Mayor. 1998. GPI-anchored proteins are organized in submicron domains at the cell surface. *Nature.* 394:798–801.

Zacharias, D.A., J.D. Violin, A.C. Newton, and R.Y. Tsien. 2002. Partitioning of lipid-modified monomeric GFPs into membrane microdomains of live cells. *Science.* 296:913–916.

Zhang, W., and L.E. Samelson. 2000. The role of membrane-associated adaptors in T cell receptor signalling. *Semin. Immunol.* 12:35–41.